Phase Segregation in SAN/PMMA Blends Probed by Rheology, Microscopy, and Inverse Gas Chromatography Techniques

M. Bousmina,*,† A. Lavoie,† and B. Riedl‡

Department of Chemical Engineering, CERSIM, and Department of Wood Science, CERSIM, Laval University, Ste-Foy, G1K 7P4 Quebec, Canada

Received January 11, 2002

ABSTRACT: Phase segregation in the poly(styrene-*co*-acrylonitrile)/poly(methyl methacrylate) (SAN/PMMA) blend with lower critical solution temperature (LCST) was assessed by linear viscoelastic rheology, optical microscopy, and inverse gas chromatography (IGC) techniques for various blend compositions. At low temperatures, the blends showed a classical behavior of homogeneous polymer melts, whereas in the vicinity of phase segregation, a shoulder in the storage modulus and in the linear relaxation modulus $G(t)$ was observed. The width of such a low-frequency/longer-time plateau and the terminal relaxation time were found to increase with temperature. Such a behavior was attributed to variable morphologies appearing at different temperatures. The development of the morphology was found to take place within a given interval of temperature rather than at a single critical temperature. Optical microscopy and IGC analyses supported the observed peculiar behavior of such a blend. Time−temperature superposition, origin of elasticity, and the Fredrickson and Larson theory were discussed in light of the obtained results.

I. Introduction

While we have gained in the past decade a deep understanding in the linear rheology and to some extent in nonlinear rheology of immiscible polymer blends, rheology in the vicinity of phase segregation remains a challenging task. This is because the measured macroscopic rheological material functions are affected by both thermodynamics and kinetics and their coupling with the applied strains and stresses. The kinetics of phase segregation is very complex and involves various mechanisms that include diffusion, nucleation, growing, and variation of size and form of the dispersed domains. This is the case for instance in binary mixtures in the neighborhood of their mixing−demixing temperature or in block copolymers in the vicinity of their order−disorder transition temperature. The key analysis of such a transient process is the fluctuation of concentration near the critical point. Consequently, most of studies in this area have focused on scattering properties during phase segregation and on spinodal decomposition. Only restricted studies have taken benefit from rheological measurements to highlight such a transition in block copolymers[1,2] and in polymer blends.[3−14] Excellent work in this area has been done by Bates for copolymers[1,2] and by Vlassopoulos, Kapnistos, and Hatzikiriakos for polymer blends.[6−12] Vlassopoulos, Kapnistos, and Hatzikiriakos et al. considered different systems under both small- and large-amplitude shear flows. The influence of large-amplitude shear flow on the phase segregation is a complex problem that implies both thermodynamics and kinetics and their coupling with the applied macroscopic external strains and stresses. Although there are many experimental facts revealing the influence of flow on phase segregation−homogenization, the modeling of such coupling is still very poor, and the behavior is, from a rigorous standpoint, not well-understood. However, much has to be gained from linear viscoelasticity where flow is presumed not to interfere with the thermodynamics and kinetics of such transition.

There are many fingerprints that can be used to infer (qualitatively or quantitatively) from rheological measurements the critical point of phase transition in polymer mixtures. One of them which is largely validated in the literature is the shoulder in the storage modulus, G', that appears in phase-segregated blends at low frequencies.[5,15−17] This can be visualized on the direct plot of G' as a function of frequency at different temperatures or on the same information plotted in terms of Cole−Cole diagram (η'' vs η'or G' as a function of G'') or in terms of relaxation spectrum that shows an additional relaxation at low frequencies. The other way is the isochrone plot of any rheological material function such as viscosity and dynamic moduli with temperature that shows a clear change of slope (depending on the system under consideration) in the vicinity of critical point.

The interest of the plot as a function of temperature is that the measurements can provide determination of spinodal decomposition temperature, T_s, using available theories.

The mean-field theory was initially worked out by Fredrickson and Larson[18] for copolymers and was extended by Ajji and Choplin[19] to the case of polymer blends. Although the theory was extended in an ad-hoc manner (no rigorous treatment was given for the discontinuities at the interface, which is valid for copolymers but questionable in the case of polymer blends), it provides a nice tool for making direct coupling between the dynamics of phase segregation−homogenization and the evolution of rheological material functions such as G' and G'' with temperature.

The purpose of this paper is to compare on a blend, made of a random copolymer of styrene and acrylonitrile (SAN) and poly(methyl methacrylate) (PMMA), the critical temperature extracted from rheological measurements with independent measurements using the

† Department of Chemical Engineering.
‡ Department of Wood Science.
* Corresponding author: Canada Research Chair on Polymer Physics and Nanomaterials. Phone: (418) 656-2769; Fax: (418) 656-5993; e-mail: Bousmina@gch.ulaval.ca.

10.1021/ma020053w CCC: $22.00
Published on Web 06/27/2002

IGC (inverse gas chromatography) technique, and direct observations using optical microscopy. The obtained results will be compared to the predictions of Fredrickson and Larson theory.[18] A critical discussion of the theory as well as the rheological signature of the phase segregation will be conducted.

II. Theoretical Background

A. Rheology. In its essence, the theory of Fredrickson and Larson[18] was worked out for homogeneous mixtures near their critical point using the time evolution of the order parameter that changes with the spatial density fluctuation. Only relaxations in the terminal zone larger than the reptation time are considered. Clearly, early stages or high frequencies in small-amplitude oscillatory shear flow that involve short chains or short segments of chains (the initial stage of diffusion that promotes phase segregation) are ignored. To calculate the extra stress generated near the critical point, the authors assume that the density pattern varies in affine manner with respect to the macroscopic applied strain. This affine variation of the density profile (or the structure factor $S(k,t)$, k being the wave vector and t the time) induces a differential change in the total free energy, $F(\gamma,t)$. The stress, $\sigma(t)$, is then calculated for small-amplitude oscillatory flow assuming an elastic response

$$\sigma(t) = \frac{\partial F(\gamma,t)}{\partial \gamma} \qquad \text{with } \lim \gamma = 0 \tag{1}$$

Detailed comments on this assumption will be given in the discussion section. Because of the elastic response and affine assumption, a periodic strain ($\gamma^* = \gamma_0 e^{i\omega t}$) induces a periodic structure factor with a lag angle = 0. Then using eq 1 and the relation $\sigma^* = G^*\gamma^*$, one finds the flowing expressions for the dynamic moduli

$$G' = \frac{k_B T\omega^2}{15\pi^2}\int_0^{k_c} \frac{k^6 {S_0}^2(k)}{\omega^2 + 4k^2 {S_0}^{-2}(k)\,\lambda^2(k)}\left[\frac{\partial {S_0}^{-1}}{\partial k^2}\right]^2 dk$$

and

$$G'' = \frac{2k_B T\omega}{15\pi^2 R}\int_0^{k_c} \frac{k^6 {S_0}^2(k)}{\omega^2 + 4k^2 {S_0}^{-2}(k)\,\lambda^2(k)}\left[\frac{\partial {S_0}^{-1}}{\partial k^2}\right]^2 dk \tag{2}$$

where S_0 is the structure factor reached at equilibrium, λ is the Onsager coefficient, and the second term in the denominator represents the squared rate of relaxation of the order parameter with a wave vector k.

To integrate eq 2, one has to know the variation of S_0 and λ with k. Ajji and Choplin[18] used the expressions given by de Gennes[19] for S_0 and by Binder[20] for λ. For binary mixtures, ${S_0}^{-1}(k)$ is given by[19]

$${S_0}^{-1}(k) = \frac{1}{\phi S_1(k)} + \frac{1}{(1-\phi)S_2(k)} - 2\chi \tag{3}$$

where S_1 and S_2 are the single-chain static coherent structure factors. For chains obeying Gaussian statistics, S_1 and S_2 can be expressed in terms of Debye function, f_D, as

$$S_i(k) = N_i f_D(x_i) \tag{4}$$

where

$$f_D(x) = \frac{2}{x^2}\{x - 1 + e^{-x}\}, \quad \text{with } x_i = k^2 {R_{gi}}^2 \tag{5}$$

R_{gi} is the radius of gyration of component i considered as an ideal chain with N_i monomers: $R_{gi} = a_i(N_i/6)^{1/2}$, with a_i being the monomer segmental length.

Under no interaction assumption (i.e., the nondiagonal Onsager coefficients vanish: $\lambda_{ij} = \lambda_{ij} = 0$), the total Onsager coefficient of the mixture $\lambda(k)$ in the long-wavelength limit is given by[20]

$$\lambda^{-1}(k) = {\lambda_{11}}^{-1}(k) + {\lambda_{22}}^{-1}(k) \tag{6}$$

where λ_{ii} is related to the diffusion coefficient, D_i, by

$$\lambda_{ii}(k) = \phi_i N_i D_i(k) = \phi_i S_i(k) {a_i}^2 W_i/N_i \tag{7}$$

where $S_i(k)$ is given by eq 4 and W_i is the rate of motion of the subunit (of length a_i) of a chain i in the total volume containing components 1 and 2. W_i of polymer melts is of order of magnitude of 10^9-10^{11} s^{-1}, and it is related to the monomeric friction coefficient ζ_i by

$$W_i = 3\pi k_B T/\zeta_i \tag{8}$$

Using eqs 3 and 6, Ajji and Choplin[18] integrated eq 2 and found the following expressions for G' and G'' in terminal one-phase region in the vicinity of critical point

$$G'(\omega) = \frac{k_B T\omega^2}{1920\pi\sqrt{18}}\left[\frac{{a_1}^2}{\phi} + \frac{{a_2}^2}{1-\phi}\right]^{1/2}\left[\frac{1}{\phi {a_1}^2 W_1} + \frac{1}{(1-\phi){a_2}^2 W_2}\right]^2 [2(\chi_s - \chi)]^{-5/2} \tag{9}$$

$$G''(\omega) = \frac{k_B T\omega}{240\pi\sqrt{18}}\left[\frac{{a_1}^2}{\phi} + \frac{{a_2}^2}{1-\phi}\right]^{-1/2}\left[\frac{1}{\phi {a_1}^2 W_1} + \frac{1}{(1-\phi){a_2}^2 W_2}\right][2(\chi_s - \chi)]^{-1/2} \tag{10}$$

where χ_s is the interaction parameter at the spinodal (${S_0}^{-1}(k{=}0) = 0$). Assuming the following expression for the interaction parameter

$$\chi = A + \frac{B}{T} \tag{11}$$

one finds the following expression

$$\left(\frac{G''^2}{TG'}\right)^{2/3} = \frac{B}{C}\left(\frac{1}{T_s} - \frac{1}{T}\right) \tag{12}$$

where C is given by

$$C = \left(\frac{45\pi}{k_\beta}\right)^{2/3}\left[\frac{{a_1}^2}{\phi} + \frac{{a_2}^2}{1-\phi}\right] \tag{13}$$

Thus, the plot of $(G''^2/G'T)^{2/3}$ vs $1/T$ provides the determination of T's.

B. Inverse Gas Chromatography (IGC). IGC is a useful technique for the study of interactions between polymers. The principle of the technique consists of the determination of residence time of a vapor probe injected at one end of a polymer packed column. The residence

time is then converted to the retention volume from which one can calculate some thermodynamic quantities (energy of interaction, Flory χ interaction parameter, solubility parameter, polar and dispersive surface energy, etc.) that reflect the interaction of the probe with the surface of the stationary polymer phase. The retention volume, V_g^0, is deduced from the retention time, Δt, by

$$V_g^0 = \Delta t J F / w \tag{14}$$

where Δt is the net retention time, that is, the difference between the retention time of the probe and the marker (methane), F the volumetric flow rate of the carrier gas, w the amount in grams of polymer on the support, and J a correction factor for gas compressibility given by

$$J = \frac{3}{2}\left[\frac{(P_i/P_o)^2 - 1}{(P_i/P_o)^3 - 1}\right] \tag{15}$$

where P_i and P_o are the inlet and outlet pressures, respectively. The net retention volume V_g^0 can be expressed conveniently as a function of the probe molecule's dispersive surface area a and its dispersive surface energy component (γ_l^d) by

$$RT \ln V_g^0 = 2Na[\gamma_l^d]^{1/2}[\gamma_s^d]^{1/2} + \text{const} \tag{16}$$

where N is Avogadro's numbers and γ_s^d is the L/W component of the solid's surface energy. Plotting [RT ln V_g^0] as a function of $[a\gamma_l^d]^{1/2}$ results in a linear function with a slope equal to γ_s^d, the nonpolar component of the solid surface energy.

III. Experimental Section

Poly(methyl methacrylate) (PMMA) was supplied by Atohaas Americas Inc., and poly(styrene−acrylonitrile)-29 (SAN-29, containing 29 wt % of acrylonitrile) was supplied by Bayer Corp. The weight-average molecular weight, M_w, and polymolecularity index, P_I, are 131 700 and 1.3 for the PMMA and 109 700 and 1.58 for the SAN29, respectively. M_w and P_I were determined by the gel permeation chromatography (GPC) system (Dawn DSP, Waters Associates) using tetrahydrofuran (THF) as the solvent and μStyragel columns with 10^6, 10^5, and 10^3 Å pore sizes at 1 mL/min flow rate. The glass transition temperatures (T_g) measured by differential scanning calorimetry (DSC, Mettler toledo star system) are 107 and 104 °C for PMMA and SAN-29, respectively.

Rheology. Blends of weight composition SAN/PMMA (10/90, 30/70, 50/50, 70/30, 90/10) were prepared by melt blending in the Haake-Büchler system 40 batch mixer at 180 °C and 50 rpm. The mixing continued until a constant torque was reached, which took about 12−15 min. The samples for rheological testing were prepared by compression molding at 200 °C in the form of 25 mm diameter disks with 1.5 mm in thickness. The viscoelastic measurements were carried out using the Rheometric Scientific controlled strain rheometer, ARES, in the parallel plates geometry. Depending on frequency and temperature, the strain was adjusted to keep the measurements in the linear regime.

Three kinds of measurements were undertaken. The first one (isothermal conditions) consisted in a frequency sweep at different temperatures ranging from 140 to 230 °C. The second one consisted in a linear relaxation experiment at various temperatures. In the third experiment, the temperature was swept from 220 to 140 °C and from 140 to 220 °C at a fixed frequency (isochronal conditions) in the linear viscoelastic zone (0.1% strain, 10 rad/s).

Inverse Gas Chromatography. All measurements were carried out on a Varian 3300 gas chromatograph equipped with a dual flame ionization detector (FID). Prepurified and dried helium was used as the carrier gas. Methane was used as marker to correct for dead volume in the column. Column inlet pressure was measured using a U-tube mercury manometer. The outlet pressure was the atmospheric pressure and was determined barometrically. Carrier gas flow rates were measured at the end of the column with a soap bubble flowmeter.

Three columns of stainless steel were prepared with a 3.2 mm inner diameter, which had been previously cleaned by methanol and tetrahydofuran (THF).

The polymers were dissolved in THF and then added on the top of the support pile without letting the solution to touch the surface, and the solvent was evaporated. Then a next portion of the solvent was applied, and the whole procedure was repeated until all the solution (including several rinsing of the solution flask) is used up. Three consecutive injections were made for each probe at each set of measurements for five different temperatures: 140, 160, 180, 200, and 220 °C. The injection of the probes volume was selected as 5 μL. The flow rate of the carrier gas, He, was set at 40 mL/min. No significant dependence of the retention volumes was noticed as a function of gas flow rate in the range (20−60 mL/min) for PMMA, SAN, and 50/50 PMMA/SAN blend.

Optical Microscopy. Morphology variation in the SAN/PMMA blend was assessed upon temperature elevation of 1 °C/min (range temperature: 100−200 °C) using an optical Axioskop (ZEISS) microscope equipped with a HS400 hot stage with a RTC1 (Instec, Inc.) temperature controller placed directly under the microscope for visual observations. The direct observations were made through a CCD camera mounted on the microscope.

IV. Results and Discussion

A. Rheology. The linear viscoelastic dynamic moduli, G' and G'', for the pure components and for the SAN/PMMA blends with weight compositions 10/90, 30/70, 50/50, 70/30, and 90/10 were measured as a function of frequency at different temperatures ranging from 140 to 230 °C by a step of 5 or 10 °C, depending on the temperature interval. For clarity purposes, the discussion in the present paper will be conducted only on blends with compositions 50/50 and 30/70. A typical example of such isotherms (G') is shown in parts a and b of Figure 1 for SAN/PMMA at compositions 50/50 and 30/70. At low temperature, the blend behaves as a homogeneous polymer melt with a rubbery plateau followed by a continuous decrease of G' as a function of frequency. Such a decrease corresponds to the beginning of the terminal zone that could not be reached at these temperatures due to the limitation of the instrument in terms of very low frequencies. In contrast, at high temperatures, the storage modulus, G', exhibits a shoulder in the low-frequency region with an increasing width with temperature. This behavior is well-documented in the literature and represents a fingerprint for the presence of phase-segregated domains that deform under the external macroscopic strain and relax due to the effect of the interfacial tension that resists to the deformation and restores the initial equilibrium shape of the domains.[15−17] Similar behavior was reported for PS/PVME blend, and the presence of the shoulder in G' was assigned to phase-separated domains of PS and PVME.[5]

To have a qualitative idea about the critical temperature or the critical zone of temperatures where the blend phase-segregates, the various isotherms were superimposed to generate a master curve at a reference temperature of 140 °C. The time−temperature super-

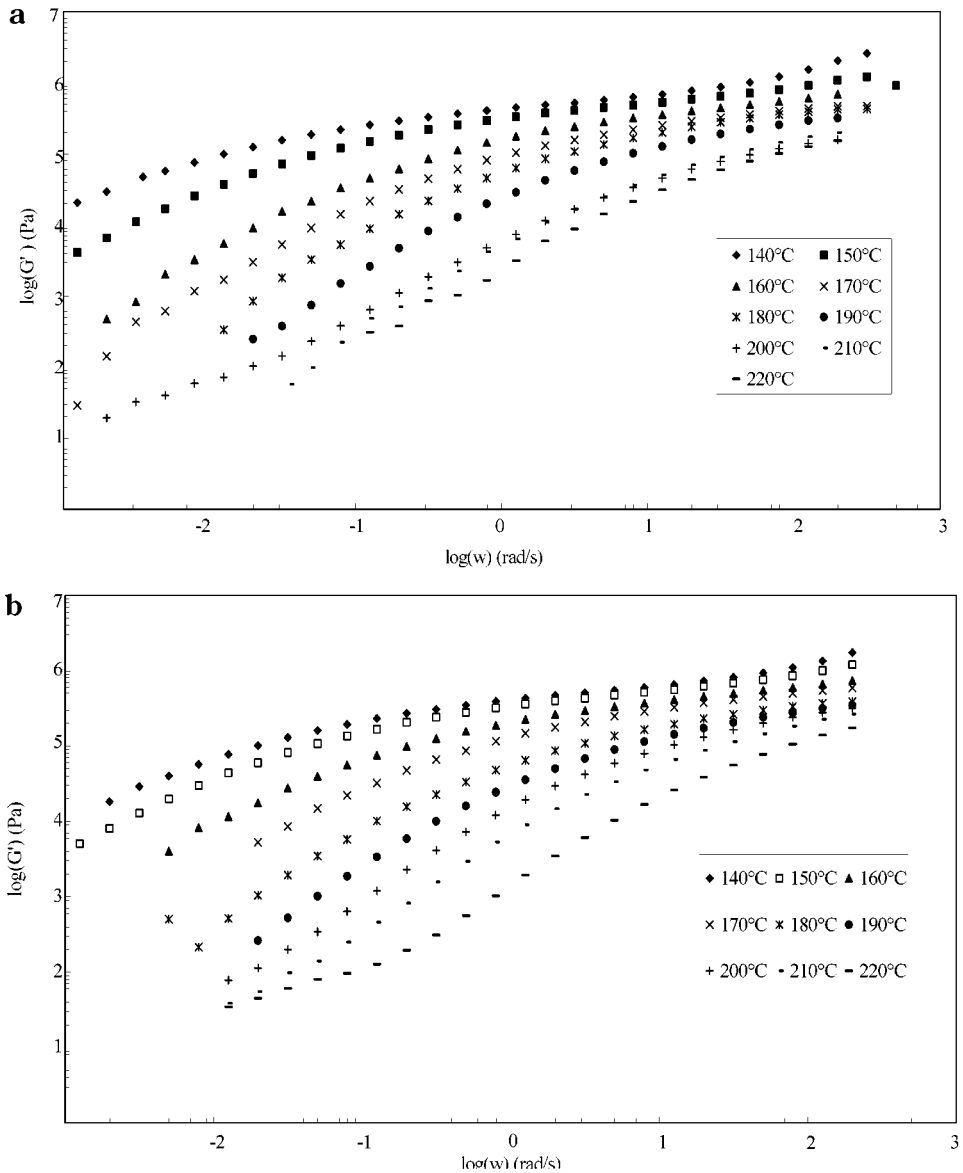

Figure 1. (a) Storage modulus at different temperatures for SAN/PMMA 50/50. (b) Storage modulus at different temperatures for SAN/PMMA 30/70.

position (TTS) principle was found to break down in the vicinity of 200 °C for 30/70 blend and in the vicinity of ($T_c = 170-200$ °C) for the 50/50 blend (Figure 2a,b). The TTS was found to work well for temperatures below and above T_c (although at higher temperatures the behavior is not thermorheologically simple), but the two obtained master curves do not superimpose.

At this stage one can suspect that the phase segregation takes place in the vicinity of T_c. To obtain the master curves, only a horizontal shift of the isotherms was needed. The WLF plot ($T - T_{ref}/\log(a_T)$) of the temperature-dependent shift factor, a_T, for 50/50 and 30/70 blends is shown in Figure 3 for a reference temperature of 140 °C. Clearly, the shift factor obeys well the WLF equation despite the failure of the TTS principle.

Shear stress relaxation experiments after a step strain (ranging in the linear regime) are depicted in Figure 4 for 30/70 at various temperatures. Clearly, the results show that at temperatures below 200 °C the relaxation of the blend is similar to that of a homogeneous polymer melt, whereas above 200 °C, the blend relaxes in the two-step regime: a fast relaxation that reflects the chains relaxation of the components and a second relaxation (secondary plateau) that describes the shape recovery of the deformed domains.

Figure 5 shows the variation of G' for SAN/PMMA blends as a function of temperature upon cooling form 230 °C to 140 °C with a rate of 1 °C/min at a frequency of 10 rad/s. The main feature to be noticed on the figure is the change in the slope of the curve with the increase of temperature. This behavior was also used by several authors[6−8] to assess the location, in terms of temperature, of the phase segregation/homogenization in polymer blends.

B. Discussion. 1. Time−Temperature Superposition Principle (TTS) in Phase-Segregating Systems. Let us first make some comments on the TTS principle in miscible/immiscible systems. Although the expressions "thermorheologically simple and thermorheologically complex" are widely used in the literature, nothing in the theory (addition or superposition of strains or stresses thorough Boltzmann equation) reflects such simplicity or complexity. Although one can

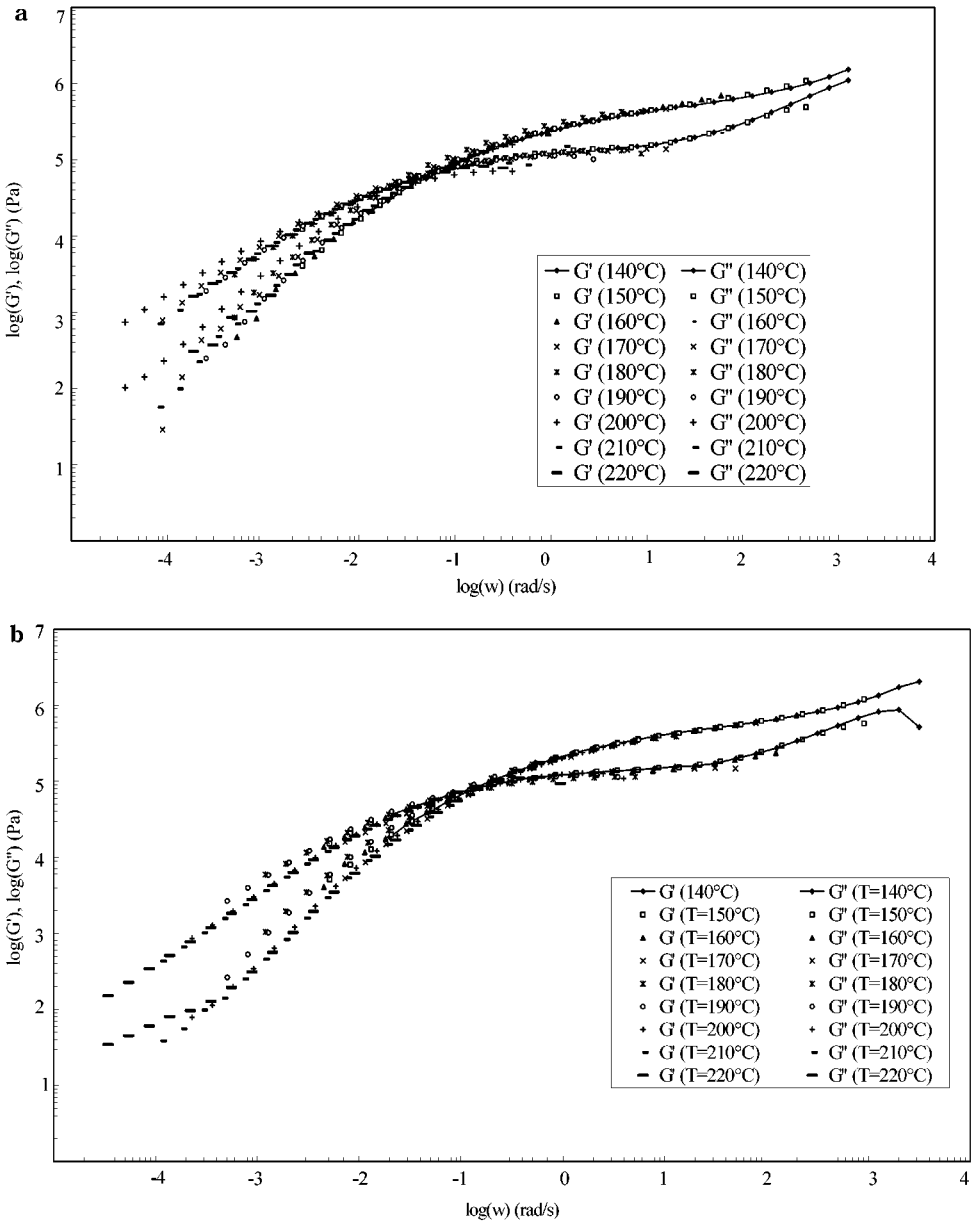

Figure 2. (a) Time−temperature superposition (TTS) principle for 50/50 SAN/PMMA blend. (b) Time−temperature superposition (TTS) principle for 30/70 SAN/PMMA blend.

find some molecular arguments in the Rouse theory for dilute solutions about the similar effects of time and temperature on the relaxation modulus, rigorously the principle in its essence is an empirical statement largely validated by experimental facts at least for amorphous polymers. The validity of TTS in a given system does not necessarily mean that the system under consideration is a homogeneous one. The only conclusion that can be made is that all relaxation mechanisms are similarly activated since, owing to TTS principle, the relaxation spectrum at two different temperatures does not change in form and in amplitude, and it is only translated on the time scale. Several results of the literature report the validity of TTS principle even for multiphase systems. Conversely, when TTS fails for mixtures of classical systems like ours, this does certainly mean some structural changes occurred in the system, and phase segregation is more likely to be considered as the cause of the failure.

When TTS works for heterogeneous systems and if the dispersed phase is highly elastic in comparison with the matrix, then one can expect a shift factor of the mixture that is dominated by the shift factor of the matrix. This can be easily understood by considering the Einstein's viscosity, η_s, of a dilute suspension of hard rigid spheres dispersed with a volume fraction ϕ in a Newtonian homogeneous medium (matrix) of viscosity η_m

$$\eta_s = \eta_m(1 + 5/2\phi)$$

By definition the shift factor, a_{Ts}, of the suspension obtained by the translation of a given material function from temperature, T, to a reference temperature, T_0, is related to the shift factor of the matrix, a_{Tm}, by

$$a_{Ts} = \log[\eta_s(T)/\eta_s(T_0)] = \log\left[\frac{\eta_m(T)}{\eta_m(T_0)}\frac{(1 + 5/2\phi)_T}{(1 + 5/2\phi)_{T_0}}\right] = \log\left[\frac{\eta_m(T)}{\eta_m(T_0)}\right] = a_{Tm} \quad (17)$$

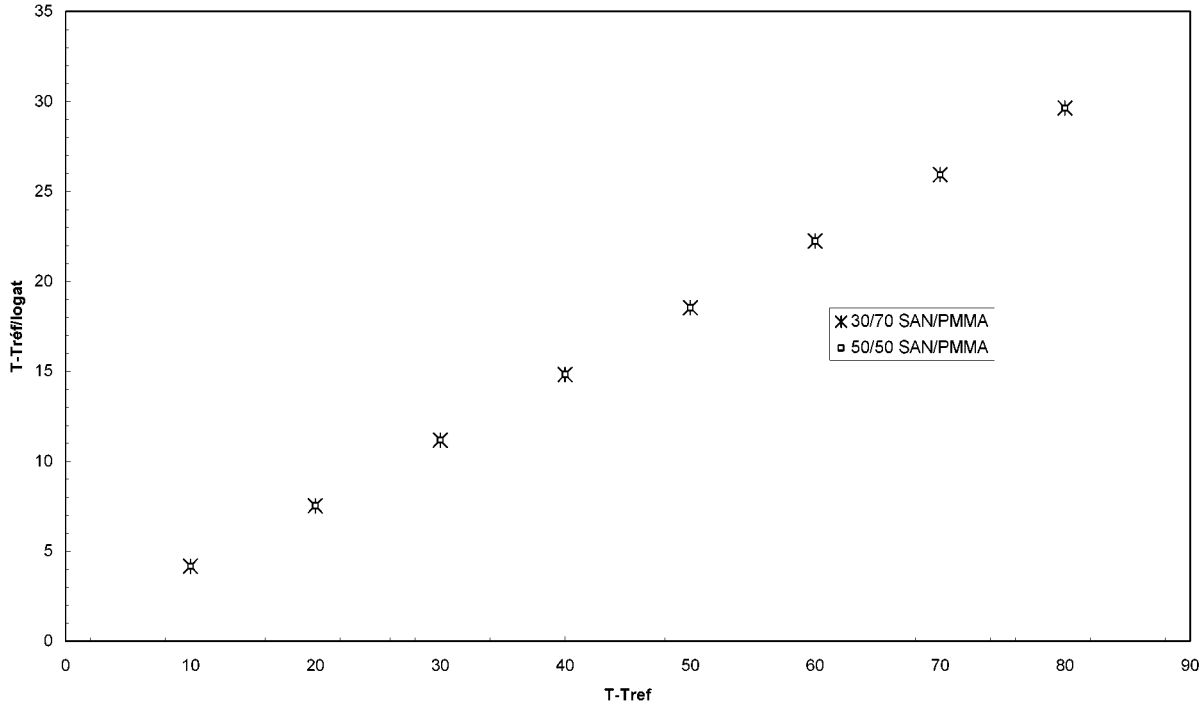

Figure 3. WLF plot of the temperature-dependent shift factor, a_T, for 50/50 and 30/70.

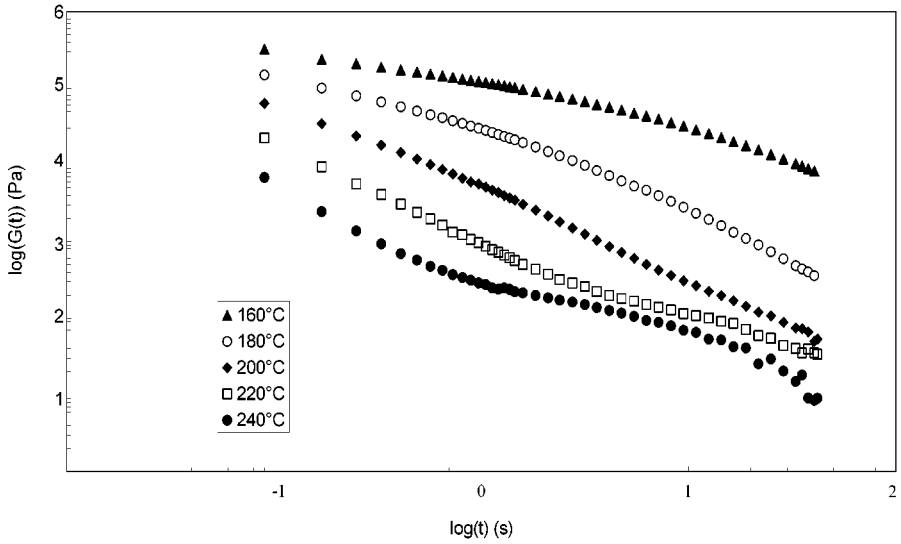

Figure 4. Linear relaxation modulus at different temperatures for SAN/PMMA 50/50.

Since the factor $(1 + 5/2\phi)$ does not depend on temperature, it comes then $a_{T\mathrm{s}} = a_{T\mathrm{m}}$. This means that when TTS works, the relaxation mechanism in suspensions (in the dilute case) is dominated by that of the matrix. For viscoelastic emulsion-type mixtures, the above relation can be substituted by a more complex equation given by the available theories such as Palierne[15] or Bousmina[16] models. In that case, $a_{T\mathrm{s}} = f(a_{T\mathrm{m}})$, where f is a complex function of the viscosity ratio and volume fraction. We should point out here that in many papers the TTS principle is confused with the WLF equation. These are two different concepts. When TTS is applied, then the variation of the determined shift factor with temperature can be represented by WLF, Arrhenius, Vogel, or other types of equations. If the plot of $(T - T_{\mathrm{ref}}/\log(a_T)$ (WLF-type equation) or $(\log(a_T)$ (Arrhenius-type equation) vs $1/T$ gives a straight line, this does not necessarily mean that TTS is valid for the system under consideration. This only means that one has in hand a good empirical correlation function (one can find other Excel or Sigma-plot type correlations) to estimate the variation of the material functions such as viscosity or dynamic moduli with temperature. In our case, although TTS does not work for our systems, we do have a nice correlation (straight line) with the WLF-type equation (Figure 4).

Using the concentration fluctuation concept, Pathak et al.[22] argued that miscible blends with dynamic symmetry, that is, the two components have closely matched glass transition temperatures and Vogel temperatures (which is the case of our system), do follow the TTS (thermorheological simplicity) principle. Their argument was based on concentration fluctuation. The estimated correlation length for concentration fluctua-

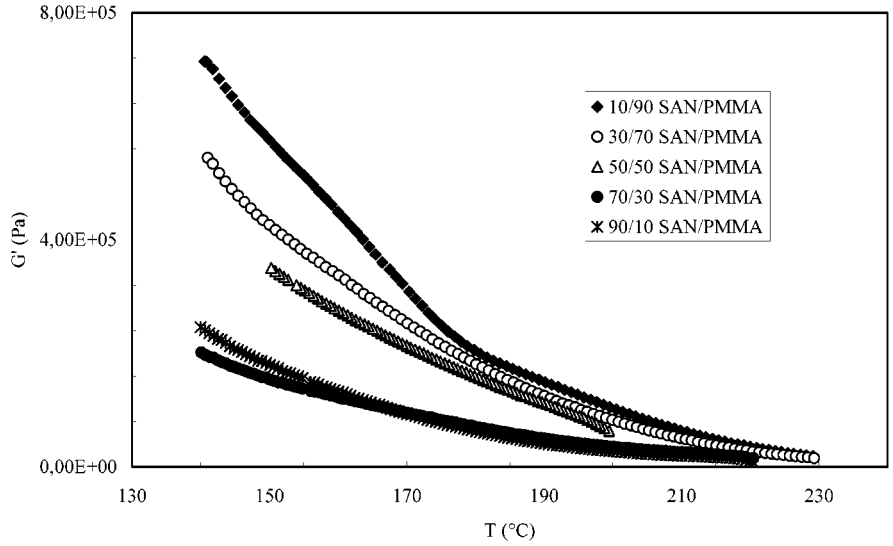

Figure 5. Storage modulus at different compositions for SAN/PMMA.

tion (from symmetric equation) in their blend was found to be of order of 20 Å. This is a rather small value, and its influence on primary rheological material functions is negligible. If this length scale was that of an interface encapsulating micronic dispersed drops, then it can be detected due to the deformation/relaxation process of the drops. Although rheological measurements are very quantitative but not at this length scale (which is approximately equivalent to 14 atoms of carbon), that is completely masked by the average bulk properties.

The situation becomes even more critical in the one-phase region but in the vicinity of phase segregation. In this case even homogeneous mixtures made of components with different degrees of polymerization, N_i, do show complex behavior. First because, as discussed before, the validity of Vogel-type equation or other type correlations for the variation of the shift factor with temperature cannot be used to judge about the validity or the failure of TTS principle. TTS and the variation of the shift factor with temperature are two distinct concepts. Second, even if the mean-field structural environment surrounding the components is the same, the stress produced by the motion of the chains of the two polymers is different due to the difference in their N_i. The motion of longer chains causes stronger stresses than shorter ones, and the classical linear division of the stress introduced by Doi and Onuki[23] has to be modified to account for the asymmetry of the polymer mixture.[24] In Doi−Onuki[23] theory, the two species 1 and 2 contribute in a linear fashion to the average velocity of the tube (tube concept)

$$\mathbf{v}_r = \mathbf{v}_T = \alpha_1 \mathbf{v}_1 + \alpha_2 \mathbf{v}_2$$

where

$$\alpha_k = \frac{\zeta_k}{\zeta_1 + \zeta_2} = \frac{\phi_k N_k}{\phi_1 N_1 + \phi_2 N_2} \tag{18}$$

The mean velocity at point **r** equals the tube velocity (tube model); v_1 and v_2 are the average velocities of components 1 and 2, respectively. ϕ_k is the volume fraction of the component k, and ζ_k is the friction coefficient of the component k with the tube surrounding it, and it is related to the monomer friction coefficient ζ_0 by

$$\zeta_k = \frac{\phi_k N_k \zeta_0}{N_e} \tag{19}$$

N_e is the average degree of polymerization between entanglement junctions. Since we have a partition of the velocity and the friction coefficients, it comes then that the stress is divided as

$$\sigma = \alpha_1 \sigma_1 + \alpha_2 \sigma_2 \tag{20}$$

However, below and near the critical point, one has to include the intermolecular interactions within the same species that will increase the friction coefficient ζ_k. This modification in ζ_k is different in components 1 and 2 due to the difference in N_i. It comes then that the asymmetry (difference in N_i) between the components affects differently the dynamics and the relaxation of the two components and thus leads to asymmetric division of stress.[24] Therefore, a Doolittle type of relaxation, $\tau \sim \tau_0 \exp[B/\epsilon_f(T - T_\infty)]$, used by Pathak et al.[22] to decide whether TTS is valid or not is not anymore acceptable due to the presence of supplementary interactions and the asymmetry of stress division.[24]

In our case, although the two components have quite identical T_g's and Vogel temperatures, the TTS fails in the vicinity of the critical temperature due to the effect of temperature activated specific interactions. Furthermore, in such phase-segregating systems, the relaxation mechanism at critical point is also affected by the apparition of the interface that induces additional relaxation of shape due to the interfacial tension (Laplace equation). In addition to the identical size and dynamics of the cooperative volumes, the interfacial relaxation makes the distribution of the concentration fluctuation nonsymmetric in the vicinity of the critical point.

2. Rheological Fingerprints of the Phase Segregation Mechanism. The increase of the width in G' and the relaxation modulus (Figures 1 and 4) and therefore the terminal relaxation time of the mixture with temperature reflect the particular variation of the macroscopic structure in the mixture. Our understand-

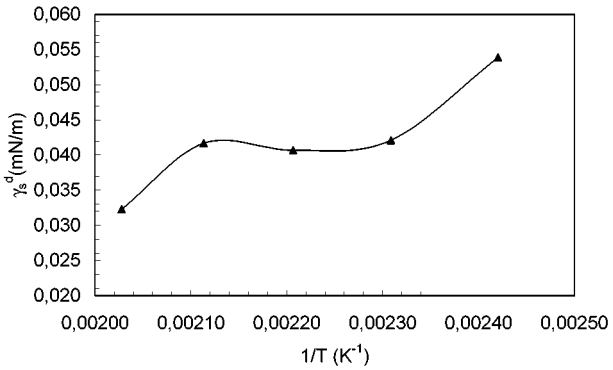

Figure 6. Variation of γ_s^d with $1/T$.

ing of linear rheology of emulsions is now quite mature, and the presence of a shoulder in G' and in $G(t)$ in the low-frequency region and in longer time interval, respectively, represents undoubtedly a signature of the presence of a macrostructure with a longer relaxation time with respect to the macromolecular relaxation times of the components. Such a relaxation time can be expressed by the following equations given by Palierne's mode,[15] τ_1, and by Bousmina's mode,[16] τ_2:

$$\tau_1 = \frac{R\eta_m}{4\alpha}\frac{(19k+16)\,[2k+3-2\phi(k-1)]}{10(k+1)-2\phi(5k+2)} \quad (21)$$

$$\tau_2 = \frac{R\eta_m}{\alpha}\frac{(k+{}^3/_2-\phi(k-1))}{1-\phi} \quad (22)$$

where α is the interfacial tension, k the viscosity ratio of the dispersed phase and the matrix, and R the average particle size of the dispersed phase. The above relations indicate that the relaxation time increases with the size of the dispersed particles. In our experiments the relaxation time increases with temperature, which means that the size of the domains in our blends increases with temperature. Our experimental results show that the phase segregation takes place in an interval of temperatures rather than at a specific critical temperature. The critical temperature determined from the variation of G' with temperature is not clearly and uniquely defined. In fact, the curve shows different discontinuities in the slope of $G'(T)$. The derivative of the curve has shown different extrema ranging in the interval 160−200 °C. Similar behavior was observed in IGC experiments. IGC results show in fact that surface phase segregation takes place over a wide interval of temperature ranging from 160 to 200 °C. We should however mention here that, above but in the vicinity of T_g, the mixture is in the rubbery state and does not flow as a Newtonian liquid, behavior that only occurs at high temperatures and in terminal zone. One therefore has to be careful to intermingle phase segregation transition with rubbery zone/terminal zone transition. In our system the particular behavior in the interval 160−200 °C is confirmed by IGC experiments (Figure 6). The variation of γ_s^d with $1/T$ shows, in fact, a clear plateau in the interval 160−200 °C. Such a behavior can be associated with different morphologies occurring in the different temperature intervals. The first stage of phase segregation occurs in the vicinity of 160 °C as was confirmed by optical microscopy (Figure 7). The kinetics of such unstable morphology is slow as was verified by time sweep experiments that did not show any change

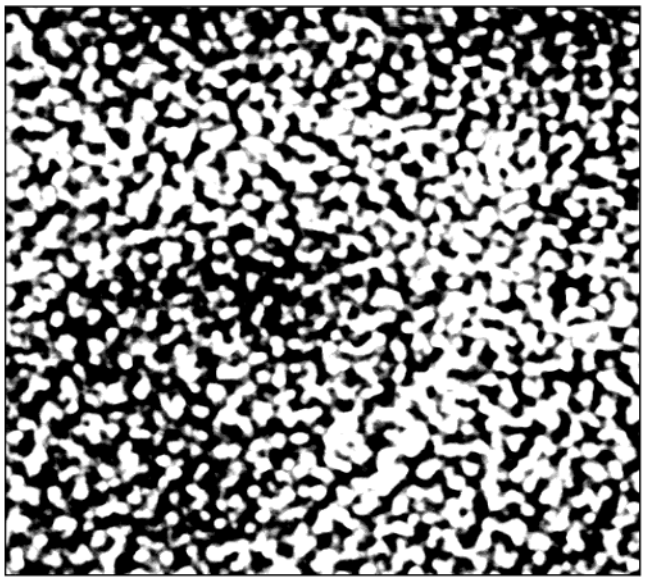

Figure 7. Typical morphology for SAN/PMMA 50/50 blend at 164 °C observed by optical microscopy.

of the dynamic moduli with time. By increasing temperature, the kinetics is accelerated (but the time of macroscopic change in the structure is very high with respect to time needed to run oscillatory shear measurements in the frequency interval 10^{-2}−10^2 rad/s), which results in the apparition of domains with larger length scale. These domains pass in the first stage through co-continuous-type structure before leading at very high temperatures to a more stable dispersed-type morphology. Such morphological variation was also observed by Kressler et al.[25] on the same system. A typical example of the first stage morphology is depicted in Figure 7. It was unfortunately not possible to quantitatively follow the whole process by microscopy due to the bad quality of the contrast between the phases.

3. Origin of Elasticity in Phase-Segregated Systems. Upon increase of temperature, one expects a decrease of the dynamic moduli due to the increase of the chain's mobility. The decrease in the slope of G' observed in Figure 6 indicates a change in the mechanism of chain dynamics. Below and in the vicinity of the first stages of phase segregation, A−A interactions in SAN and PMMA phases become dominant, leading to thermodynamic phase segregation. The temperature variation of the blend lies above the straight line that indicates the linear decrease of $G'(T)$ that would occur if the blend was a homogeneous melt. Vlassopoulos et al.[6−9] argued that such an increase in elasticity originates from the concentration fluctuation, and it is a result of the coupling between thermodynamics and mobility forces in the vicinity of phase segregation. Although the argument is pertinent regarding the concentration fluctuation, the variation of mobility or relaxation at the microscopic level (macromolecular level) is only a secondary cause for the increase in the elasticity. In fact, during nucleation and phase separation, the interface comes into play, which introduces a supplementary elasticity in the system due to the deformation and the shape recovery of the formed domains (macroscopic level). This has the same origin as the increase of elasticity at low frequencies observed on the isotherm of G' vs frequency (or on $G(t)$). The interfacial tension (Laplace forces) is the motor for a such mechanism, and this elasticity has nothing to do

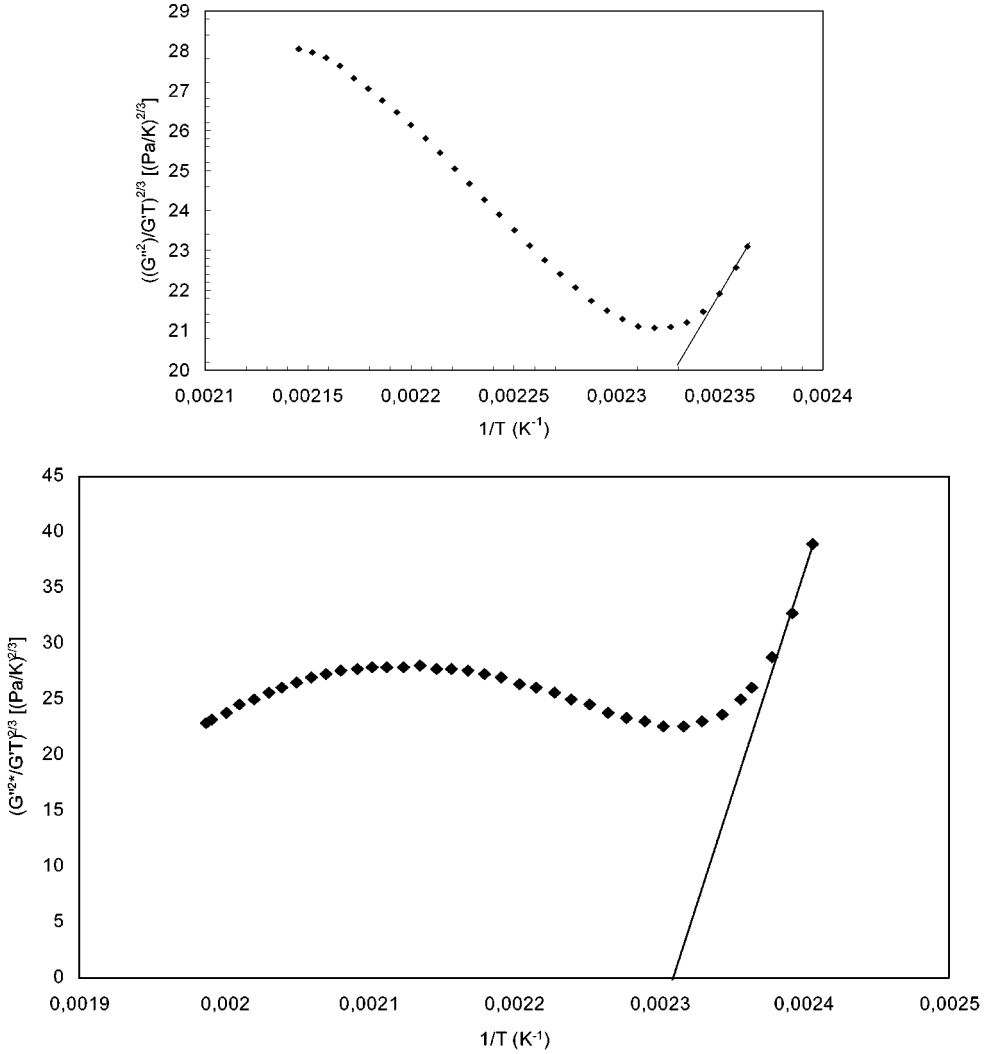

Figure 8. (a) Determination of critical temperature for 50/50 SAN/PMMA blend using eq 12. (b) Determination of critical temperature for 30/70 SAN/PMMA blend using eq 12.

Table 1. Critical and Spinodal Temperatures (°C) for Phase Segregation in 50/50 SAN/PMMA Blend Determined by Various Techniques

T_c (°C) from the onset for the shoulder in G', $G(t)$	T_c (°C) from the failure of TTS	T_s (°C) from Fredrickson and Larson plot	T_s (°C) from IGC	T_c, T_s (°C) from optical microscopy
200	170−200	160	160	160

with the elasticity evoked in the mean field theory of the Fredrickson and Larson theory.

4. Comparison with the Fredrickson and Larson Theory. To work out their model, Fredrickson and Larson[17] considered the relaxation in the terminal zone larger than the reptation timed. Clearly, early stages or high frequencies in small-amplitude oscillatory shear flow that involve short chains or short segments of chains (the initial stage of diffusion that promotes phase segregation) are ignored. The authors start their calculations by considering an oscillatory shear flow under a small amplitude of strain assuming an elastic response (see eq 1). Rigorously, this contradicts the first assumption. In fact, viscoelastic materials respond elastically only in the high-frequency region (or for short times of loading). For times larger than the reptation time, polymer melts behave rather as viscous liquids! Ajji and Choplin[18] also evaluated the equations of Fredrickson and Larson[17] (eq 2) in the terminal zone for times higher than the reptation time. To do such evaluation, they used a weighted average structure factor S_i (see eq 3) corrected by the term -2χ as was given by de Gennes.[19] However, the term of interaction is absent in eq 6 for the total Onsager coefficient that was assumed to be a simple average of the individual Onsager coefficients of the components. This means that the mutual diffusion coefficient is just a weighted average of the diffusion coefficients of the components, which is obviously not correct for interacting systems.[26] The absence of the interaction parameter in eq 6 introduces a large error on the scaling relation since the variation of the quantity $(G''^2/G'T)^{2/3}$ with temperature is a consequence of the variation of the interaction parameter, χ, with temperature. The noninteraction assumption is also implicit in the choice of the rate of motion, W_i, of the subunits. Although it was not mentioned in their paper,[18] the equations implicitly suppose that W_{ij} is identical to W_i. This means that the friction coefficient of species 1 in the mixture of 1 and 2 is equivalent to the friction coefficient of species 1 in its own melt. This is of course not true and a fortiori in the vicinity of phase segregation. In reference to the

above discussion, the theory provides only as a rough estimation of the critical point.

To use the theory, one has to carry out experiments as a function of T at low frequencies in the terminal zone of one-phase mixture in the vicinity phase transition. Clearly, this restricts the choice of model systems to verify the theory, unless one can perform very low-frequency experiments at transition temperature or use model systems that rapidly show a terminal zone at the vicinity of phase transition. Unfortunately, neither such a rheometer facility nor such a model system is known yet. Only what one can do is a rough use of the theory.

A typical plot of $(G''^2/G'T)^{2/3}$ vs $1/T$ is shown in Figure 8a,b for 50/50 and 30/70 blends. The slope of the curve is taken in the low-temperature zone, and the intercept with the $1/T$ axis gives a priori the temperature of spinodal decomposition, T_s. This technique has been successfully used by Vlassopoulos et al.[6−8] to assess the spinodal decomposition in various LCST and USCT blends. In our experiments only a limited interval of temperatures was explored in the homogeneous region due to the proximity to T_g.

The critical temperatures and spinodal decomposition temperature determined by the different techniques are summarized in Table 1. The critical temperature extracted from the shoulder in the storage modulus, G', or in the relaxation modulus is about 30−40 °C higher than the critical temperature obtained by other measurements. The shoulder in frequency sweep experiments ($G'(\omega)$) or in relaxation experiments ($G(t)$) reflects the deformation−relaxation process of the dispersed domains. At the beginning of phase separation, the domains are very small, and their relaxation occurs at frequencies (or times) that might lie in the frequency range or time interval of the relaxation of the pure phases. The relaxation of the dispersed domains is therefore hindered by the relaxation of the pure components, and in this case the small-amplitude oscillatory shear or relaxation experiments are not sensitive enough to detect the phase separation. The insensitivity of dynamic oscillatory shear measurements has also been reported in some polymer blends modified by a small amount of specific copolymers.[27] Upon increase of temperature, the domains become of larger size, and then the relaxation time (or the shoulder in $G'(\omega)$ and in $G(t)$) as given by eqs 21 and 22 becomes higher and then measurable. This may explain the higher value of critical temperature determined from the shoulder in $G'/G(t)$. The results obtained by other techniques (IGC, TTS, and optical microscopy) are quite similar.

V. Concluding Remarks

In this work we have shown that linear rheology is a useful tool to assess the critical point of phase segregation in polymer blends. The results obtained on the SAN/PMMA system showed however that phase segregation occurs in an interval of temperature with the morphology varying from co-continuous to dispersed-type structure. The rheological results were found to be in rough agreement with independent measurements obtained by IGC and optical microscopy analysis. Particular discussion was given on the TTS principle and the origin of elasticity in the vicinity of phase segregation. The increase of elasticity originates from the deformation/relaxation of the interface. Contrary to what was reported in the literature, our experimental results have shown that although the two polymers have close Vogel temperatures, the TTS principle was found to break down in the vicinity of the critical temperature. Despite the failure of TTS, the WLF-type equation was found to perfectly fit the dependency of the shift factor on the temperature (linear variation).

Acknowledgment. This work was financially supported by the NSERC (Natural Sciences and Engineering Research Council of Canada), Canada Research Chair on Polymer Physics and Nanomaterials, and the FCAR (Fonds pour la Formation de Chercheurs et l'Aide de la Recherche du Québec) funds.

References and Notes

(1) Bates, F. S. *Macromolecules* **1984**, *17*, 2607.
(2) Rosedale, J. H.; Bates, F. S. *Macromolecules* **1990**, *23*, 2329.
(3) Ajji, A.; Choplin, L.; Prud'homme, R. *J. Polym. Sci.*. **1988**, *26*, 2279.
(4) Mani, S.; Malone, M. F.; Winter, H. H. *J. Rheol.* **1992**, *36*, 1625.
(5) Carreau, P. J.; Bousmina, M.; Ajji, A. Rheological Properties of Blends. Facts and Challenges. In *Pacific Polymers*; Springer-Verlag: New York, 1994.
(6) Vlassopoulos, D. *Rheol. Acta* **1996**, *35*, 556.
(7) Kapnistos, M.; Vlassopoulos, D.; Anastasiadis, S. H. *Europhys. Lett.* **1996**, *34*, 513.
(8) Kapnistos, M.; Hinrichs, A.; Vlassopoulos, D.; Anastasiadis, S. H.; Stammer, A.; Wolf, B. A. *Macromolecules* **1996**, *29*, 7155.
(9) Vlassopoulos, D.; Koumoutsakos, A.; Anastasiadis, S. H.; Hatzikiriakos, S. G.; Englezos, P. *J. Rheol.* **1997**, *41*, 739.
(10) Chopra, D.; Vlassopoulos, D.; Hatzikiriakos, S. G. *J. Rheol.* **1998**, *42*, 1227.
(11) Chopra, D.; Haynes, C.; Hatzikiriakos, S. G.; Vlassopoulos, D. *J. Non-Newtonian Fluid Mech.* **1999**, *82*, 367.
(12) Chopra, D.; Vlassopoulos, D.; Hatzikiriakos, S. G. *J. Rheol.* **2000**, *44*, 27.
(13) Vinckier, I.; Laun, H. M. *Rheol. Acta* **1999**, *38*, 274.
(14) Madbouly, S. A.; Ougizawa, T.; Inoue, T. *Macromolecules* **1999**, *32*, 5631.
(15) Palierne, J. F. *Rheol Acta* **1990**, *29*, 2204; Erratum **1991**, *30*, 349.
(16) Bousmina, M. *Rheol. Acta* **1999**, *38*, 73.
(17) Bousmina, M. *Rheol. Acta* **1999**, *38*, 251.
(18) Fredrickson, G. H.; Larson, R. G. *J. Chem. Phys.* **1987**, *86*, 1553. Larson, R. G.; Fredrickson, G. H. *Macromolecules* **1987**, *20*, 1897.
(19) Ajji, A.; Choplin, L. A. *Macromolecules* **1991** *24*, 5221.
(20) De Gennes, P.-J. *J. Chem. Phys.* **1980**, *72*, 4756; *Scaling Concepts in Polymer Physics*; Cornell University Press: Ithaca, NY, 1979.
(21) Binder, K. *J. Chem. Phys.*. **1983**, *70*, 6387.
(22) Pathak, J. A.; Colby, R. H.; Kamath, S. Y.; Kumar, S. K.; Stadler, R. *Macromolecules* **1998**, *31*, 8988.
(23) Doi, M.; Onuki, A. *J. Phys. (Paris)* **1992**, *II2*, 1631.
(24) Tanaka, H. *Phys. Rev. E* **1997**, *56*, 4451.
(25) Kressler, J.; Kammer, H. W.; Klostermann, K. *Polym. Bull. (Berlin)* **1986**, *15*, 113.
(26) Qiu, H.; Bousmina, M. *Macromolecules* **2000**, *17*, 6588.
(27) Iza, M.; Bousmina, M. *Rheol. Acta* **2001**, *39*, 232.

MA020053W